

# Novel insights into charge and spin pairing instabilities in nanoclusters

A. N. Kocharian<sup>1</sup>, G. W. Fernando<sup>2</sup>, K. Palandage<sup>2</sup> and J. W. Davenport<sup>3</sup>

<sup>1</sup>*Physics Dept., California State University, Los Angeles, CA 90032*

<sup>2</sup>*U-46, Physics Dept., University of Connecticut, Storrs, CT 06269 and*

<sup>3</sup>*Computational Science Center and Center for Functional Nanomaterials, Brookhaven National Laboratory, Upton, NY 11973*

Electron pairing and ferromagnetism in various cluster geometries are studied with emphasis on tetrahedron and square pyramid under variation of interaction strength, electron doping and temperature. These exact calculations of charge and spin collective excitations and pseudogaps yield intriguing insights into level crossing degeneracies, phase separation and condensation. Criteria for spin-charge separation and reconciliation driven by interaction strength, next nearest coupling and temperature are found. Phase diagrams resemble a number of inhomogeneous, coherent and incoherent nanoscale phases seen recently in high  $T_c$  cuprates, manganites and CMR nanomaterials.

PACS numbers: 65.80.+n, 73.22.-f, 71.10.Fd, 71.27.+a, 71.30.+h, 74.20.Mn

## I. INTRODUCTION

Systems with correlated electrons display a rich variety of physical phenomena and properties: different types of magnetic ordering, (high- $T_c$ ) superconductivity, ferroelectricity, spin-charge separation, formation of spatial inhomogeneities [1, 2, 3, 4, 5, 6] (phase separation, stripes, local gap and incoherent pairing, charge and spin pseudogaps). The realization of these properties in clusters and bulk depends on interaction strength  $U$ , doping, temperature, the detailed type of crystal lattice and sign of coupling  $t$  [7]. Studies of perplexing physics of electron behavior in non-bipartite lattices encounter enormous difficulties. Exact solutions at finite temperatures exist only in a very few cases [9, 10, 11]; perturbation theory is usually inadequate while numerical methods have serious limitations, such as in the Quantum Monte-Carlo method and its notorious sign problem. On the contrary, one can get important insights from the exact solutions for small clusters (“molecules”). For example, squares or cubes are the building blocks, or prototypes, of solids with bipartite lattices, whereas triangles, tetrahedrons, octahedrons without electron-hole symmetry may be regarded as primitive units of typical frustrated systems (triangular, pyrochlore, perovskite). Exact studies of various cluster topologies can thus be very useful for understanding nanoparticles and respective bulk systems. One can take a further step and consider an inhomogeneous bulk system as a collection of many such decoupled clusters, which do not interact directly, but form a system in thermodynamic equilibrium [11, 12, 13]. Thus we consider a collection of such “molecules”, not at fixed average number of electrons per each cluster, but as a grand canonical ensemble, for fixed chemical potential  $\mu$ . The electrons can be splintered apart by spin-charge separation due to level crossings driven by  $U$  or temperature, so that the collective excitations of electron charge and spin of different symmetries can become quite independent and propagate incoherently. We have found that local charge and spin density of states or corresponding susceptibilities can have different pseudogaps which

is a sign of spin-charge separation. For large  $U$  near half filling, holes prefer to be localized on separate clusters having Mott-Hubbard (MH) like charge pseudogaps [13] and Nagaoka ferromagnetism (FM) [7]; otherwise, spin density waves or spin liquids may be formed. At moderate  $U$ , this approach leads to reconciliation of charge and spin degrees with redistribution of charge carriers or holes between square clusters. The latter, if present, can signal a tendency toward phase separation, or, if clusters “prefer” to have two holes, it can be taken as a signature of pairing [8]. This, in turn, could imply imposed opposite spin pairing followed by condensation of charge and spin degrees into a BCS-like coherent state. Although this approach for large systems is only approximate, it nonetheless gives very important clues for understanding large systems whenever correlations are local. We have developed this approach in Refs. [12, 13, 14, 15, 16] and successfully applied to typical unfrustrated (linked squares) clusters. Our results are directly applicable to nanosystems which usually contain many clusters, rather well separated and isolated from each other but nevertheless being in thermodynamic equilibrium with the possibility of having inhomogeneities for different number of electrons per cluster. Interestingly, an ensemble of square clusters displays “checkerboard” patterns, nanophase inhomogeneity, incoherent pairing and nucleation of pseudogaps [1, 2, 3, 4, 5]. The purpose of this work is to further conduct similar extensive investigations in frustrated systems [17], exemplified by 4-site tetrahedrons and 5-site square pyramids. As we shall see, certain features in various topologies are quite different and these predictions could be exploited in the nanoscience frontier by synthesizing clusters or nanomaterials with unique properties [18].

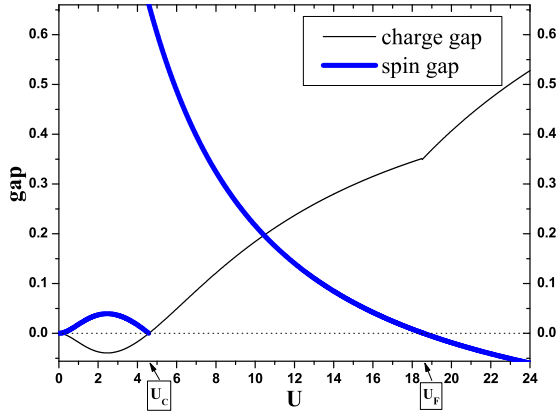


FIG. 1: Charge  $\Delta^c$  and spin  $\Delta^s$  gaps versus  $U$  in an ensemble of squares at  $\langle N \rangle \approx 3$  and  $T = 0$ . Phase A: Charge and spin pairing gaps of equal amplitude at  $U \leq U_c$  describe bose condensation of electrons similar to BCS-like coherent pairing with a single energy gap. Phase B: Mott-Hubbard like insulator at  $U_c < U < U_F$  leads to  $S = \frac{1}{2}$  spin liquid behavior. Phase C: Parallel (triplet) spin pairing ( $\Delta^s < 0$ ) at  $U > U_F$  displays  $S = \frac{3}{2}$  saturated ferromagnetism (see Sec. III A).

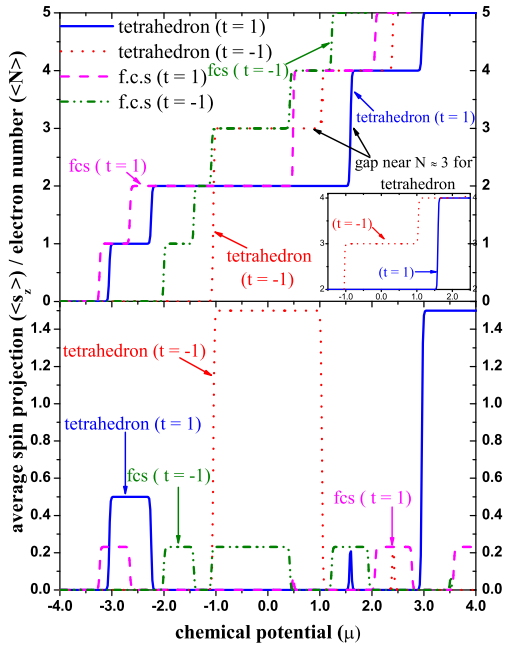


FIG. 2:  $\langle N \rangle$  and  $\langle s_z \rangle$  versus  $\mu$  in grand canonical ensemble of tetrahedrons and fcs at  $U = 4.0$ ,  $T = 0.01$  and  $h = 0.1$ . Mott-Hubbard like ferromagnetism for  $\langle s_z \rangle = \frac{3}{2}$  at  $\langle N \rangle = 3$  in tetrahedron occurs for  $t = -1$ , while absence of charge pseudogap near  $\langle N \rangle \approx 3$  metallic state with spin rigidity manifests level crossing degeneracy related to pairing (see inset).

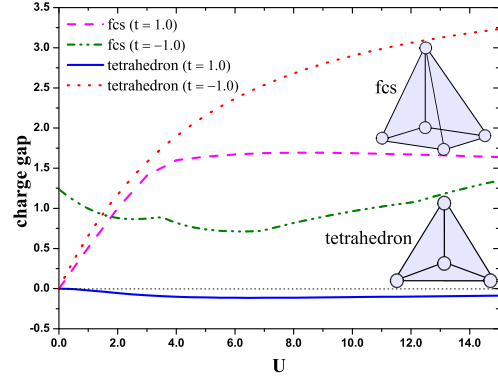


FIG. 3:  $\Delta^c$  versus  $U$  for one hole off half filling in tetrahedrons and fcs at  $T = 0$ . In tetrahedron,  $\Delta^c < 0$  at  $t = 1$  implies phase separation and coherent pairing with  $\Delta^s \equiv \Delta^P$ , while  $\Delta^c > 0$  for  $S = \frac{3}{2}$  at  $t = -1$  leads to a ferromagnetic insulator ( $\Delta^s < 0$ ) for all  $U$ . In fcs,  $\Delta^c > 0$  at  $\langle N \rangle \approx 4$  for  $t = \pm 1$  describes Mott-Hubbard like antiferromagnetism ( $\Delta^s > 0$ ).

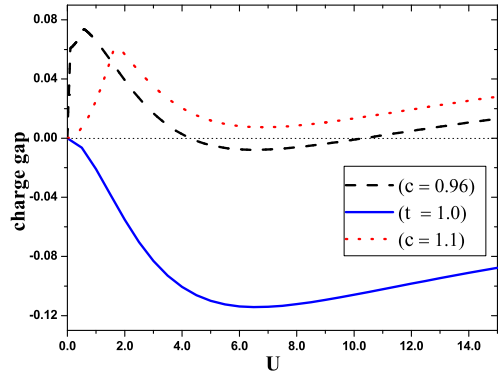


FIG. 4:  $\Delta^c$  versus  $U$  at  $\langle N \rangle = 3$  and  $T = 0.01$  in tetrahedron ( $t = 1$ ) and deformed tetrahedral clusters ( $c = 0.96$  and  $1.1$ ). Charge and spin pairing gaps of equal amplitude at  $t = 1$  imply coherent pairing, while  $\Delta^c > 0$  and  $\Delta^s < 0$  at  $c = 1.1$  correspond to an unsaturated ferromagnetic insulator for  $S = \frac{1}{2}$ . Coherent pairing is retained in a narrow range near  $c \approx 1$ .

## II. MODEL AND FORMALISM

Exact diagonalization of the Hubbard model (HM)

$$H = -t \sum_{\langle ij \rangle \sigma} c_{i\sigma}^\dagger c_{j\sigma} + U \sum_i n_{i\uparrow} n_{i\downarrow}, \quad (1)$$

and quantum statistical calculations of charge  $\chi_c$  and spin  $\chi_s$  susceptibilities, i.e., *fluctuations*, in a grand canonical ensemble and pseudogaps  $\Delta^c(T) = E(N+1) + E(N-1) - 2E(N)$  and  $\Delta^s(T) = E(S+1) - E(S)$

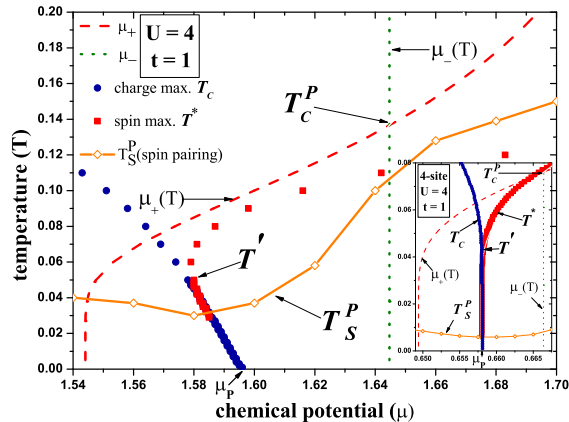


FIG. 5: The  $T$ - $\mu$  phase diagram of tetrahedrons without electron-hole symmetry at optimally doped  $\langle N \rangle \approx 3$  regime near  $\mu_P = 1.593$  at  $U = 4$  and  $t = 1$  illustrates the condensation of electron charge and onset of phase separation for charge degrees below  $T_C^P$ . The incoherent phase of preformed pairs with unpaired opposite spins exists above  $T_S^P$ . Below  $T_S^P$ , the paired spin and charge coexist in a coherent pairing phase. The charge and spin susceptibility peaks, denoted by  $T^*$  and  $T_c$ , define pseudogaps calculated in the grand canonical ensemble, while  $\mu_+(T)$  and  $\mu_-(T)$  are evaluated in canonical ensemble. Charge and spin peaks reconcile at  $T' \geq T \geq T_S^P$ , while  $\chi^c$  peak below  $T_S^P$  signifies metallic (charge) liquid (see inset for square cluster and Ref. [15]).

TABLE I: Ground state (GS) in various cluster geometries for one hole off half filling at large  $U = 900$  and  $t = \pm 1$  having saturated ferromagnetism (SF), unsaturated ferromagnetism (UF), antiferromagnetism (AF) or coherent pairing (CP).

cluster type	$N_a$	$N$	$S$	$\Delta^s$	$\Delta^c$	$t$	GS
triangle	3	2	1	-0.998	3.011	-1	SF
tetrahedron/nnn square	4	3	1.5	-0.997	3.987	-1	SF
square pyramid/fcs	5	4	2	-0.417	2.596	-1	SF
square	4	3	1.5	-0.262	1.15	$\pm 1$	SF
triangle	3	2	0	1.008	1.993	1	AF
tetrahedron/nnn square	4	3	0	0.002	-0.002	1	CP
square pyramid/fcs	5	4	1	-0.115	1.543	1	UF

for canonical energies  $E(N)$  and  $E(S)$  ( $N$  and  $S$  being the total number of electrons and spin respectively) yield valuable insights into quantum critical points and various phase transitions as shown in Ref. [13]. By monitoring the peaks in  $\chi^c$  and  $\chi^s$  one can identify charge/spin pseudogaps and relevant crossover temperatures; nodes, sign and amplitude of pseudogaps determine energy level crossings, phase separation, electron pairing ranges, spin-charge separation and reconciliation regions.

### III. RESULTS

#### A. Bipartite clusters

For completeness and to facilitate the comparison with frustrated clusters, we first summarize the main results obtained earlier for small  $2 \times 2$  and  $2 \times 4$ -sites bipartite clusters in Refs. [12, 13, 14, 15]. The energies are measured in units  $|t| = 1$  in all results that follow. Fig. 1 illustrates  $\Delta^c$  and  $\Delta^s$  in ensemble of  $2 \times 2$  square clusters at  $\langle N \rangle \approx 3$  and  $T \rightarrow 0$ . Vanishing of gaps indicates energy (multiple) level crossings and corresponding quantum critical points,  $U_c$  and  $U_F$ . The negative gaps show phase separations for charge below  $U_c = 4.584$  and spin degrees above  $U_F = 18.583$  [11, 12]. Phase A: Negative charge gap below  $U_c$  displays electron pairing  $\Delta^P = |\Delta^c|$  and charge phase separation into hole-rich (charged) metal and hole-poor (neutral) cluster configurations. In a grand canonical approach  $\Delta^s > 0$  at  $U \leq U_c$  corresponds to electron charge redistribution with opposite spin (singlet) pairing. This picture for electron charge and spin gaps of equal amplitude  $\Delta^s \equiv \Delta^P = -\Delta^c$  of purely electronic nature at  $\langle N \rangle \approx 3$  is similar to the BCS-like coherency in the attractive HM and will be called coherent pairing (CP). In equilibrium, the spin singlet background ( $\chi_s > 0$ ) stabilizes phase separation of paired electron charge in a quantum CP phase. The unique gap  $\Delta^s \equiv \Delta^P$  at  $T = 0$  in Fig. 1 is consistent with the existence of a single quasiparticle energy gap in the BCS theory for  $U < 0$  [19]. Positive spin gap in Fig. 1 at  $U < U_c$  provides pairs rigidity in response to a magnetic field and temperature (see Sec. III C). However, unlike in the BCS theory, the charge gap differs from spin gap as temperature increases. This shows that coherent thermal excitations in the exact solution are not quasiparticle-like renormalized electrons, as in the BCS theory, but collective paired charge and coupled opposite spins. The spin gap  $\Delta^s$  for excited  $S = \frac{3}{2}$  configuration in Fig. 1 above  $U_c$  is shown for canonical energies in a stable MH-like state,  $\Delta^c > 0$ . Phase B: Unsaturated ferromagnetism (UF) for unpaired  $S = \frac{1}{2}$  with zero field  $\chi^s$  peak for gapless  $s_z = \pm \frac{1}{2}$  projections and gapped  $\Delta^s > 0$  for  $S = \frac{3}{2}$  excitations at  $U_c \leq U \leq U_F$  will be called a spin liquid. Phase C: Negative  $\Delta^s < 0$  at  $U > U_F$  defines  $S = \frac{3}{2}$  saturated ferromagnetism (SF). Localized holes at  $\Delta^c > 0$  rule out possible Nagaoka FM in a metallic phase [7]. Field fluctuations lift  $s_z$ -degeneracy and lead to segregation of clusters into magnetic domains.

It appears that the ensemble of square clusters share common and important features with larger bipartite clusters in the ground state and at finite temperatures [19] (see Sec. III C). For example, in  $2 \times 4$  ladders (Fig. 5 of Ref. [15]), we have identified the existence of (negative and positive) oscillatory behavior in  $(T = 0)$  charge gaps as a function of  $U$ . Similar to what was seen in square clusters at low temperatures, we observe level crossing degeneracies in charge and spin sectors in bipar-

tite  $2 \times 4$  clusters at relatively small and large  $U$  values, respectively. Thus the use of chemical potential and departure from zero temperature singularities in the canonical and grand canonical ensembles appear to be essential for understanding important physics related to the pseudogaps, phase separation, pairings and corresponding crossover temperatures. A full picture of coherent and incoherent pairing, electronic inhomogeneities and magnetism emerges only at finite, but rather low temperatures. (If we set  $t = 1$  eV, the most of the interesting physics is seen to occur below a few hundred degrees K.)

### B. Tetrahedrons and square pyramids

The topology of the tetrahedron is equivalent to that of a square with next nearest neighbor coupling ( $t' = t$ ) while the square pyramid of the octahedral structure in the HTSCs is related to face centered squares (fcs). The average electron number  $\langle N \rangle$  and magnetization  $\langle s^z \rangle$  versus  $\mu$  in Fig. 2 for  $T = 0.01$  shows contrasting behavior in pairing and magnetism at  $t = 1$  and  $t = -1$  for the tetrahedron at  $\langle N \rangle = 3$  and fcs at  $\langle N \rangle = 4$ . Different signs of  $t$  in these topologies for one hole off half filling lead to dramatic changes in the electronic structure. Fig. 3 illustrates the charge gaps at small and moderate  $U$ . Tetrahedron at  $t = -1$ : SF with a negative spin gap in a MH-like phase exists for all  $U$ . Tetrahedron at  $t = 1$ : metallic CP phase with charge and spin gaps of equal amplitudes similar to the BCS-like pairing, discussed for squares in Sec. III A, forms at all  $U$ . FCS at  $t = -1$ : MH-like insulator displays two consecutive crossovers at  $U \simeq 6.89$  from ( $S = 0$ ) antiferromagnetism (AF) into ( $S = 1$ ) UF and into ( $S = 2$ ) SF above  $U = 12.19$ . FCS at  $t = 1$ : MH-like insulator shows crossover at  $U \simeq 29.85$  from ( $S = 0$ ) AF into ( $S = 1$ ) UF. In triangles, SF and AF are found to be stable for all  $U > 0$  at  $t = -1$  and  $t = 1$  respectively. Finally Table I illustrates magnetic phases at large  $U$  and  $T = 0$ . For example, the squares and all frustrated clusters at  $t = -1$  exhibit stable SF; Tetrahedron and triangle at  $t = 1$  retain CP and AF respectively; UF for the  $S = 1$  state, separated by  $\Delta^s = -0.115$  from  $S = 0$ , exists in fcs at  $t = 1$ . Fig. 4 shows charge gap at two coupling values  $c$  between the vertex and base atoms in the deformed tetrahedron. Vanishing of gap, driven by  $c$ , manifests level crossings for  $c = 0.96$ , while  $c = 1.1$  and  $t = 1$  cases describe a single phase with avoided crossings.

### C. Phase diagrams

Fig. 5 illustrates a number of nanophases, defined in Refs. [13, 15], for the tetrahedron similar to bipartite clusters. The curve  $\mu_+(T)$  below  $T_c^P$  signifies the onset of charge paired condensation. As temperature is lowered below  $T^*$ , a spin pseudogap is opened up first, as seen in NMR experiments [15], followed by the gradual disappearance of the spin excitations, consistent with the sup-

pression of low-energy excitations in the HTSCs probed by STM [3, 4, 5]. The opposite spin CP phase with fully gapped collective excitations begins to form at  $T \leq T_s^P$ . The charge inhomogeneities [1, 2] of hole-rich and charge neutral *spinodal* regions between  $\mu_+$  and  $\mu_-$  are similar to those found in the squares and resemble important features seen in the HTSCs. Fig. 5 shows the presence of bosonic modes below  $\mu_+(T)$  and  $T_s^P$  for paired electron charge and opposite spin respectively. This picture suggests condensation of electron charge and spin at various crossover temperatures while condensation in the BCS theory occurs at a single  $T_c$  value. The temperature driven spin-charge separation above  $T_s^P$  resembles an incoherent pairing (IP) phase seen in the HTSCs [2, 3, 4, 5]. The charged pairs without spin rigidity above  $T_s^P$ , instead of becoming superconducting, coexist in a nonuniform, charge degenerate IP state similar to a ferroelectric phase [19]. The unpaired weak moment, induced by a field above  $T_s^P$ , agrees with the observation of competing dormant magnetic states in the HTSCs [4]. The coinciding  $\chi^s$  and  $\chi^c$  peaks at  $T_s^P \leq T \leq T'$  show full reconciliation of charge and spin degrees seen in the HTSCs above  $T_c$ . In the absence of electron-hole symmetry, the tetrahedral clusters near optimal doping  $\mu_P$  undergo a transition with temperature from a CP phase into a MH-like phase.

## IV. CONCLUSION

It is clear that our exact results, discussed above, provide novel insight into level crossings, spin-charge separation, reconciliation and full bose condensation [20]. Separate condensation of electron charge and spin degrees offers a new route for superconductivity, different from the BCS scenario. The electronic instabilities found for various geometries, in a wide range of  $U$  and temperatures, will be useful for the prediction of electron pairing, ferroelectricity [19] and possible superconductivity in nanoparticles, doped cuprates, etc. [1, 2, 3, 4, 5, 6]. In contrast to the squares, exact solution for the tetrahedron exhibits coherent and incoherent pairings for all  $U$ . Our findings at small, moderate and large  $U$  carry a wealth of new information at finite temperatures in bipartite and frustrated nanostructures regarding phase separation, ferromagnetism and Nagaoka instabilities in manganites/CMR materials. These exact calculations illustrate important clues and exciting opportunities that could be utilized when synthesizing potentially high- $T_c$  superconducting and magnetic nanoclusters assembled in two and three dimensional geometries [18]. Ultra-cold fermionic atoms in an optical lattice [21] may also offer unprecedented opportunities to test these predictions.

We thank Daniil Khomskii, Valery Pokrovsky for helpful discussions and Tun Wang for valuable contributions. This research was supported in part by U.S. Department of Energy under Contract No. DE-AC02-98CH10886.

- 
- [1] Y. Kohsaka *et al.*, *Science* **315**, 1380 (2007).  
[2] T. Valla *et al.*, *Science* **314**, 1914 (2006).  
[3] A. C. Bóia, R. Laihob and E. Lähderantab, *Physica C* **411**, 107 (2004).  
[4] H. E. Mohottala *et al.*, *Nature Materials* **5**, 377 (2006).  
[5] K. K. Gomes *et al.*, *Nature* **447**, 569 (2007).  
[6] R. Moro, S. Yin, X. Xu, and W. A. de Heer, *Phys. Rev. Lett.* **93**, 086803 (2004); X. Xu, S. Yin, R. Moro, and W. A. de Heer, **95**, 237209 (2005).  
[7] Y. Nagaoka, *Phys. Rev.* **147**, 392 (1966).  
[8] S. Belluci, M. Cini, P. Onorato, and E. Perfetto, *J. Phys.: Condens. Matter* **18**, S2115 (2006); W-F. Tsai and S.A. Kivelson, *Phys. Rev.* **B73**, 214510 (2006); S.R. White, S. Chakravarty, M.P. Gelfand, and S.A. Kivelson, *ibid* **B45**, 5062 (1992); R.M. Fye, M.J. Martins, and R.T. Scalettar, *ibid* **42**, R6809 (1990); N.E. Bickers, D.J. Scalapino, and R.T. Scalettar, *Int. J. Mod. Phys. B* **1**, 687 (1987).  
[9] H. Shiba and P. A. Pincus, *Phys. Rev.* **B5**, 1966 (1972).  
[10] L. M. Falicov and R. H. Victora, *Phys. Rev.* **B30**, 1695 (1984).  
[11] R. Schumann, *Ann. Phys.* **11**, 49 (2002); **17**, 64 (2008).  
[12] A. N. Kocharian, G. W. Fernando, K. Palandage and J. W. Davenport, *J. Magn. Magn. Mater.* **300**, 585 (2006).  
[13] A. N. Kocharian, G. W. Fernando, K. Palandage, and J. W. Davenport, *Phys. Rev.* **B74**, 024511 (2006).  
[14] A. N. Kocharian, G. W. Fernando, K. Palandage, and J. W. Davenport, *Phys. Lett.* **A364**, 57 (2007).  
[15] G. W. Fernando, A. N. Kocharian, K. Palandage, Tun Wang, and J. W. Davenport, *Phys. Rev.* **B75**, 085109 (2007).  
[16] K. Palandage, G. W. Fernando, A. N. Kocharian, and J. W. Davenport, *Journal of Computer-Aided Materials Design* **14**, 103 (2007).  
[17] I. A. Sergienko and S. H. Curnoe, *Phys. Rev.* **B70**, 144522 (2004).  
[18] S. Y. Wang, J. Z. Yu, H. Mizuseki, Q. Sun, C. Y. Wang, and Y. Kawazoe, *Phys. Rev.* **B70**, 165413 (2004).  
[19] A. N. Kocharian, G. W. Fernando, K. Palandage, and J. W. Davenport, to be published (2008).  
[20] R. Friedberg, T. D. Lee, and H. C. Ren, *Phys. Rev.* **B50**, 10190 (1994).  
[21] J. K. Chin *et al.*, *Nature* **443**, 961 (2006).